LETTERS
PUBLISHED ONLINE: 16 JANUARY 2011 | DOI: 10.1038/NPHYS1879
nature physics

Observation of a ubiquitous three-dimensional superconducting gap function in optimally doped $Ba_{0.6}K_{0.4}Fe_2As_2$

Y-M. Xu[1], Y-B. Huang[2,3], X-Y. Cui[3], E. Razzoli[3,4], M. Radovic[3,4], M. Shi[3], G-F. Chen[5], P. Zheng[2], N-L. Wang[2], C-L. Zhang[6], P-C. Dai[2,6,7], J-P. Hu[2,8], Z. Wang[1] and H. Ding[2]*

The iron-pnictide superconductors have a layered structure formed by stacks of FeAs planes from which the superconductivity originates. Given the multiband and quasi three-dimensional[1] (3D) electronic structure of these high-temperature superconductors, knowledge of the quasi-3D superconducting (SC) gap is essential for understanding the superconducting mechanism. By using the k_z capability of angle-resolved photoemission, we completely determined the SC gap on all five Fermi surfaces (FSs) in three dimensions on $Ba_{0.6}K_{0.4}Fe_2As_2$ samples. We found a marked k_z dispersion of the SC gap, which can derive only from interlayer pairing. Remarkably, the SC energy gaps can be described by a single 3D gap function with two energy scales characterizing the strengths of intralayer Δ_1 and interlayer Δ_2 pairing. The anisotropy ratio Δ_1/Δ_2, determined from the gap function, is close to the *c*-axis anisotropy ratio of the magnetic exchange coupling J_c/J_{ab} in the parent compound[2]. The ubiquitous gap function for all the 3D FSs reveals that pairing is short-ranged and strongly constrains the possible pairing force in the pnictides. A suitable candidate could arise from short-range antiferromagnetic fluctuations.

Angle-resolved photoemission spectroscopy (ARPES) has played an important role in revealing the electronic structure of the pnictides. These measurements have typically been carried out at a fixed incident photon energy ($h\nu$) and varying incident angles that map out the planar band dispersion as a function of k_x and k_y. Thus far, four FS sheets have been observed with two hole pockets centred around the Γ (0, 0) point and two electron pockets around the M (π, 0) point in the unfolded 2D Brillouin zone. Below the superconducting transition temperature T_c, nodeless SC gaps open everywhere on the FS sheets[3–6], pointing to a pairing order parameter with an *s*-wave symmetry in the *a*–*b* plane, in agreement with a number of theoretical results[7–11]. However, there are other experiments that have indicated possible nodes in the superconducting gap of some pnictides, either line nodes in the *a*–*b* plane or nodes along the *c* axis[12–14]. It is well known that on tuning the incident photon energy $h\nu$, the allowed direct transitions will shift in energy and, consequently, in the momentum perpendicular to the *a*–*b* plane (k_z), which enables the determination of the electronic dispersion along the *c* axis.

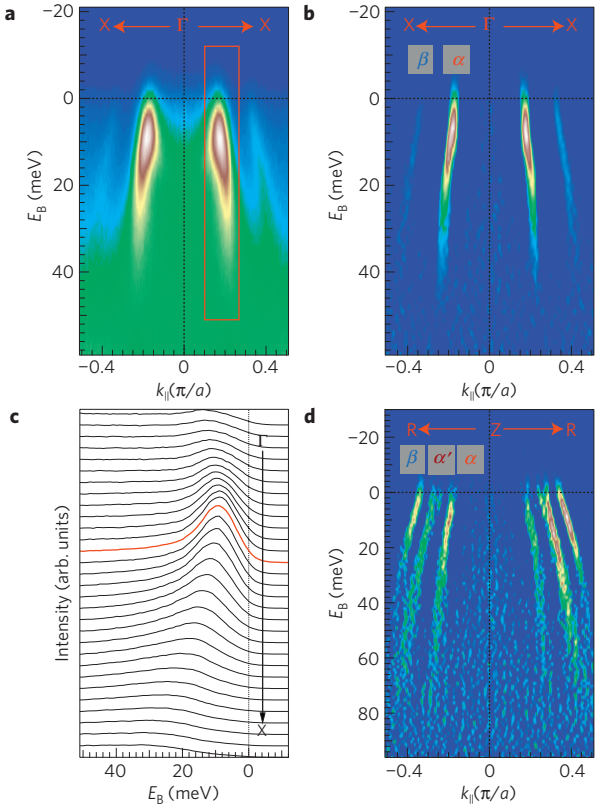

Figure 1 | Band dispersion of superconducting $Ba_{0.6}K_{0.4}Fe_2As_2$. a, ARPES spectral intensity measured at 10 K plotted on a false-colour scale as a function of the in-plane momentum ($k_{||}$) and binding energy along Γ–X using 46-eV photons, which corresponds to $k_z = 0$. Two hole-like bands (α (inner) and β (outer)) are observed. **b**, Second derivative of the spectral intensity plot as shown in **a**. **c**, A set of EDCs within the *E*–*k* range indicated by the red rectangle in **a**. The red EDC is at k_F of the α band. **d**, Second derivative plot of the dispersion along Z–R ($k_z = \pi$) measured using 32-eV photons. Three hole-like bands (α (inner), α' (middle) and β (outer)) are observed.

[1]Department of Physics, Boston College, Chestnut Hill, Massachusetts 02467, USA, [2]Beijing National Laboratory for Condensed Matter Physics, and Institute of Physics, Chinese Academy of Sciences, Beijing 100190, China, [3]Swiss Light Source, Paul Scherrer Institute, CH-5232 Villigen, Switzerland, [4]Laboratory for Synchrotron and Neutron Spectroscopy, EPF Lausanne, CH-1015 Lausanne, Switzerland, [5]Department of Physics, Renmin University of China, Beijing 100872, China, [6]Department of Physics and Astronomy, The University of Tennessee, Knoxville, Tennessee 37996, USA, [7]Neutron Scattering Sciences Division, Oak Ridge National Laboratory, Oak Ridge, Tennessee 37831, USA, [8]Department of Physics, Purdue University, West Lafayette, Indiana 47907, USA. *e-mail: dingh@aphy.iphy.ac.cn.

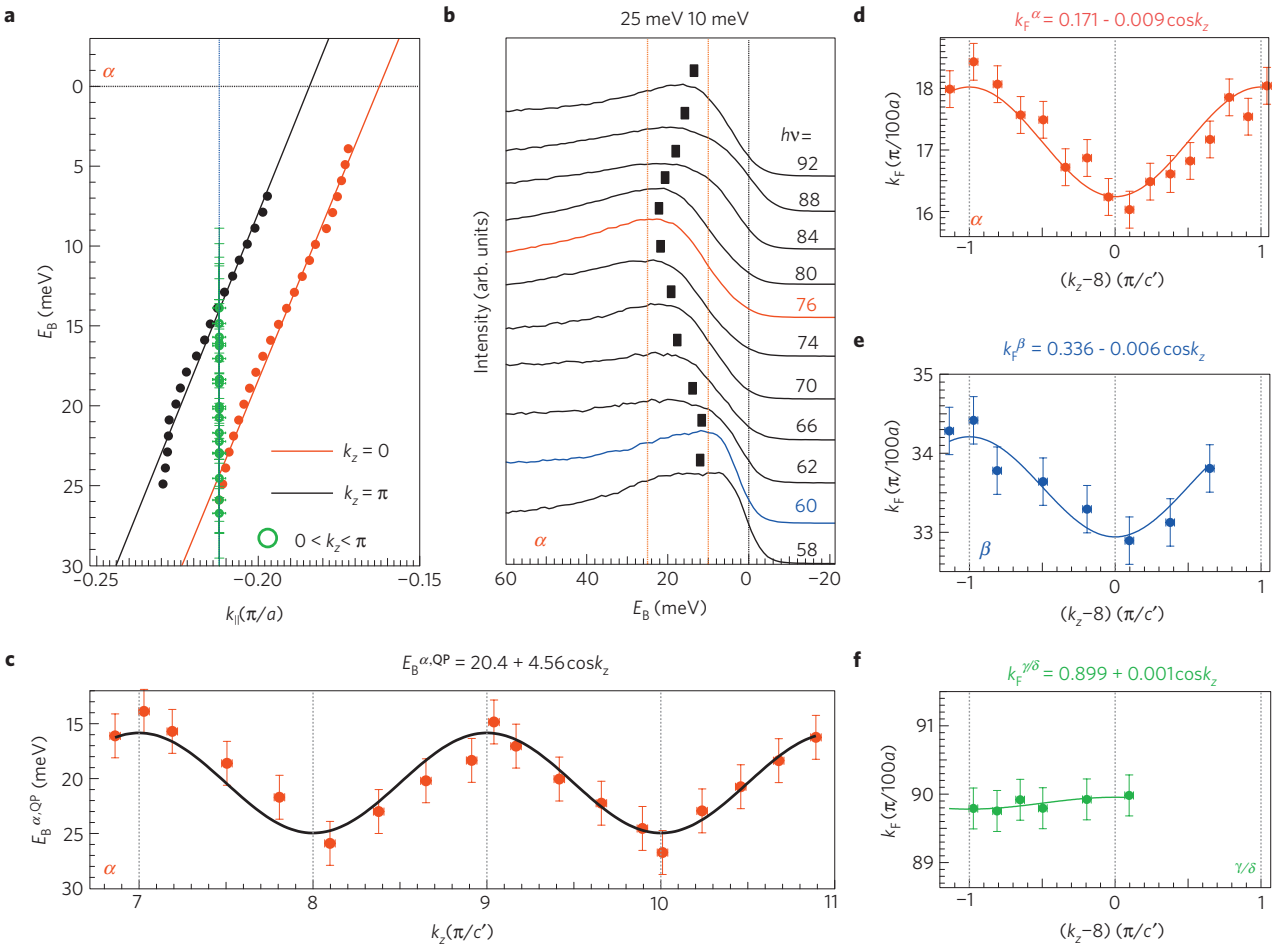

Figure 2 | k_z dispersion of quasiparticles and Fermi surface warping. a, Comparison of the α band dispersions at $k_z = 0$ (red dots) and $k_z = \pi$ (black dots) extracted from the peak position of momentum distribution curves along Γ–X. The solid lines are linear fits to the corresponding dispersions. The green dots denote the binding energies of the quasiparticle peak of the α band as shown in **b** measured at a fixed $k_{||}$ (slightly below k_F) using different photon energies (or different k_z). **b**, Corresponding EDCs to the green dots shown in **a**. The black vertical bars indicate the binding energies of the quasiparticle (QP) peaks. The red (blue) EDC corresponds to $k_z = 0$ ($k_z = \pi$). Note that the 'shoulder' at the higher binding energy (~20 meV) of the EDC measured at $h\nu = 58$ eV is from the α' band. **c**, k_z dispersion of the α band extracted from **a** and **b**. The solid curve is the fit using $\cos k_z$. **d**, k_z dependence of the in-plane k_F of the α-FS parallel to Γ–X. The solid curve is the $\cos k_z$ fit. **e**,**f**, Same as **d**, but for the β-FS and electron-like (γ/δ)-FS. The error bars in **a** and **c** are standard deviations of the Lorentzian fit to the coherent peaks. The error bars of k_F in **d**,**e** and **f** are standard deviations of the Lorentzian fit to MDC peaks at the Fermi energy. The error bars of k_z in **c**,**d**,**e** and **f** are obtained from the estimated uncertainty of the inner potential (~±1 eV) according to $k_z = \sqrt{2m[(h\nu - \phi - E_B)\cos^2\theta + V_0]}/\hbar$.

In the free-electron final-state approximation, the conversion is given by $k_z = \sqrt{2m[(h\nu - \phi - E_B)\cos^2\theta + V_0]}/\hbar$, where V_0 is an experimentally determined inner potential[15]. Several earlier ARPES studies have used this k_z-resolving capability to probe the 3D dispersion of the normal-state electronic structure in $BaFe_2As_2$-based pnictides, and found a large k_z band dispersion in the orthorhombic phase in the vicinity of the parent compound[16–20]. The 3D nature of the superconducting gap, which is critically important to the understanding of pnictide superconductivity, has yet to be studied.

Figure 1a shows the spectral intensity measured at 10 K at a photon energy of 46 eV, which corresponds to the reduced $k_z = 0$ (see discussion below), plotted as a function of the binding energy and in-plane momentum along the Γ–X direction. Two hole-like bands are clearly observed, corresponding to the α (inner) and β (outer) bands respectively, in both the spectral intensity plot and the second derivative intensity plot (Fig. 1b). The energy distribution curves (EDCs) show that the α band disperses towards the Fermi level (E_F) and bends back (Fig. 1c) as a result of the opening of the superconducting gap of ~12 meV, consistent with earlier ARPES experiments[3,6]. When the photon energy is tuned to 32 eV ($k_z = \pi$), in addition to the α and β bands observed around the zone centre (the Z point), a third hole-like band (Fig. 1d) emerges between the α and β bands. Although the band calculations[21–23] have predicted the existence of the third hole-like band in the pnictides, mostly for the 1111 pnictides, there is no accurate prediction of the observed k_z dispersion of this band for the 122 compound. We label this new band as the α' band, the full dispersion and Fermi surface of which will be described in a separate paper.

Comparing Fig. 1b and d quantitatively, it is clear that the α band dispersion undergoes a parallel shift in binding energy under different photon energies, as shown in Fig. 2a. Moreover, this modulation exhibits a well-defined periodicity in the photon energy, indicating that the excess energy is carried by the coherent interlayer quasiparticle tunnelling with well-defined momentum k_z. Converting the photon energy into momentum k_z with an inner potential of 15 eV (ref. 16), we find that the periodicity in k_z is remarkably close to that expected from the lattice spacing between the adjacent Fe layers, that is, $2\pi/c' = 0.951$ Å^{-1}, with $c' = c/2 = 6.6$ Å (due to bilayer FeAs in $Ba_{0.6}K_{0.4}Fe_2As_2$; ref. 24).

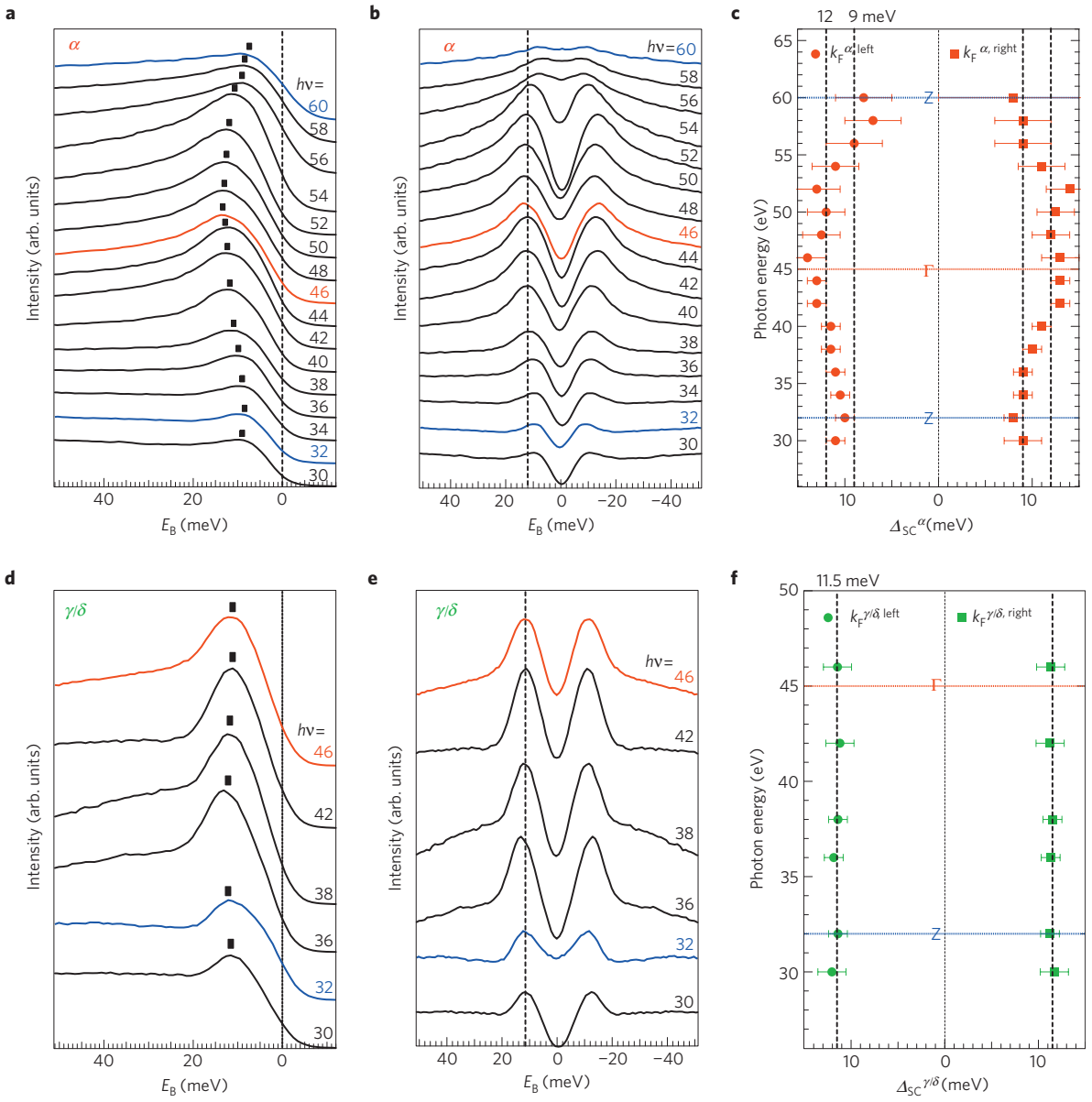

Figure 3 | k_z dependence of the superconducting gaps. a, Photon-energy-dependent EDCs measured at the left k_F on the α-FS along Γ–X or its parallel directions with different k_z. Red (blue) EDCs correspond to $k_z = 0$ ($k_z = \pi$). The black blocks indicate the binding energies of the coherent peaks. **b**, Corresponding symmetrized EDCs of the ones shown in **a**. The dashed line at 12 meV is a guide to the eyes for viewing the variation of the SC gap at different $h\nu$. **c**, Extracted values of the SC gap (defined as the half value of peak-to-peak positions in the symmetrized EDCs) on the α-FS at different photon energies. The dots (squares) are obtained from the left (right) side of k_F on the α-FS. **d**–**f**, Same as **a**–**c** but on the electron-like FSs (γ/δ) along Γ–M or its parallel directions. The dashed line in **e** is at 11.5 meV as a guide to the eyes for viewing the SC gap at different $h\nu$. The error bars are twice the derivation of the Lorentzian fit to coherent peaks.

To determine the k_z dispersion of the α band, we stay at a fixed in-plane momentum such that the binding energy varies in a region sufficiently away from the SC gap, and plot the quasiparticle dispersion (Fig. 2b) as a function of k_z, as shown in Fig. 2c. The dispersion can be described remarkably well by

$$E_{3D}{}^{\alpha}(k_x, k_y, k_z) = E_{2D}{}^{\alpha}(k_x, k_y) + 2t_{\perp}\cos k_z \qquad (1)$$

with an interlayer hopping amplitude $t_{\perp} \simeq 2.3$ meV in the binding energy range around 20 meV (along the Γ–X direction). Here and hereafter, for notational simplicity, k_x, k_y, k_z carries the units of $1/a, 1/b, 1/c'$, respectively. The k_z dispersion results in the warping of the α-FS sheet along k_z. One important implication of the observed k_z dispersion is that this band cannot be a surface state, which would have no k_z dispersion. To describe the underlying FS quantitatively, we extrapolate the fitted dispersion given in equation (1) to the Fermi level and display the in-plane Fermi wave vector (k_F) along Γ–X for the α, β and the electron-like (γ/δ) bands as a function of k_z in Fig. 2d–f, respectively. The FS area variation (defined as δ in $(1 \pm \delta)A_{FS}$) in the a–b plane is ∼10%, 4% and 1% for the α, β and γ/δ bands, respectively, with the same periodicity along k_z.

Having established the k_z dispersion of the quasi-3D electronic structure, we turn to the k_z dependence of the SC gaps on different FS sheets obtained using many photon energies. Figure 3a shows a collection of the EDCs at the Fermi crossings of the α band for different photon energies $h\nu$ = 30–60 eV. Appreciable gap

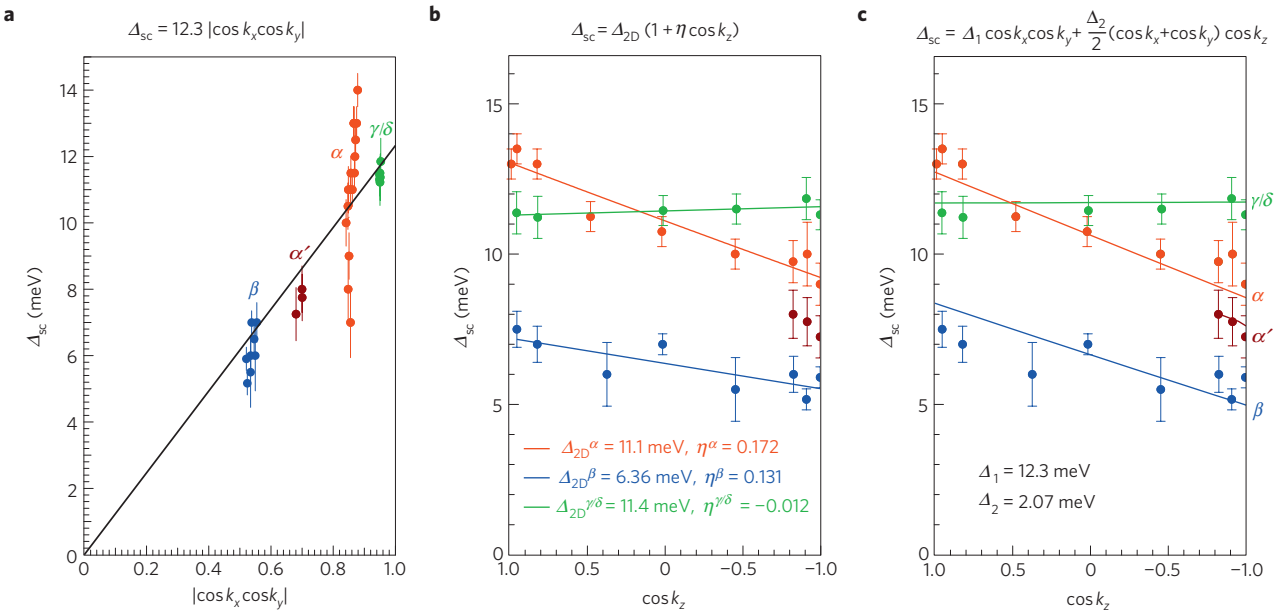

Figure 4 | 3D superconducting gap function $\Delta(k_x, k_y, k_z)$. **a**, The SC gap values on the α-FS (red dots), β-FS (blue dots), γ/δ-FS (green dots) and α'-FS (brown dots) as functions of $|\cos k_x \cos k_y|$. The black solid line is the gap function $|\Delta| = \Delta_0 |\cos k_x \cos k_y|$, with $\Delta_0 = 12.3$ meV. **b**, Same as **a** but as functions of $\cos k_z$. The solid lines are independent linear fits to the SC gaps on the different FS sheets using a generic 3D gap function $|\Delta(k_x, k_y, k_z)| = |\Delta_{2D}(k_x, k_y)(1+\eta\cos k_z)|$. **c**, Same as **b** but using a single 3D gap function $|\Delta(k_x, k_y, k_z)| = |\Delta_1 \cos k_x \cos k_y + (\Delta_2/2)(\cos k_x + \cos k_y)\cos k_z|$, with $\Delta_1 = 12.3$ meV and $\Delta_2 = 2.07$ meV, to fit all the SC gaps. The error bars are standard deviations of the measured SC gaps.

variations are clearly visible in the symmetrized EDCs in Fig. 3b. The extracted SC gap values (defined as $\Delta_{3D}{}^{\alpha}$) at both left and right Fermi crossings are plotted in Fig. 3c as a function of the photon energy (left axis) and c-axis momentum k_z (right axis). Remarkably, $\Delta_{3D}{}^{\alpha}$ shows rather large periodic variations from ~9 to ~13 meV, then back to ~9 meV as k_z moves from Z to Γ and back to Z. A similar k_z dependence of the smaller SC gap on the β band is also observed, varying from ~5 to ~7 meV, as shown later in Fig. 4. However, the k_z variation of the SC gap on the electron-like (γ/δ)-FS sheets is much smaller, as indicated in Fig. 3d–f, where the Bogoliubov quasiparticle peak is shown to remain at a nearly constant energy of ~11.5 meV as k_z varies from Γ to Z. We note that an appreciable k_z dependence of pairing strength associated with the 3D band structure has been predicted in this material[25], although the predicted certain in-plane anisotropy and gap nodes have not been observed in our experiments.

It is interesting to note that the observed gap values (Fig. 3c,f) and the FS warping (Fig. 2d,f) along k_z are anti-correlated; that is, when the in-plane FS area at a fixed k_z becomes larger (smaller) the SC gap becomes smaller (larger) on the same plane. At first glance, one might conclude that the gap variation along k_z originates predominantly from the tunnelling-induced FS warping, that is, the k_z dependence of the in-plane Fermi vector k_F, as is implied by the simplest form of an in-plane $s\pm$ gap function $\Delta_{s\pm} = \Delta_0 \cos k_x \cos k_y$. However, this turns out not to be the case. The <10% change in the in-plane Fermi vector is too small to account for the large, near 40%, gap variations because of the small 'gap velocity' in the pnictides. This is clearly seen from Fig. 1, where the near doubling of the Fermi vector in going from the α-FS to the β-FS results only in a gap change from 12 to 6 meV. To illustrate this point further, we plot in Fig. 4a the measured gap values as a function of $|\cos k_x \cos k_y|$ at the Fermi points for the α, α', β, and the electron (γ/δ) bands. Notice that although the average gap value follows this 2D form, the marked deviations induced by the k_z dispersion could indicate that the pairing is not purely 2D and that there is a further driving force, namely, the pairing between the layers, that is predominantly responsible for the gap dispersion with k_z.

For an anisotropic layered superconductor with interlayer coupling, we adopt a simple form of the gap function,

$$\Delta_{3D}(k_x, k_y, k_z) = \Delta_{2D}(k_x, k_y)(1+\eta\cos k_z) \qquad (2)$$

This is a direct generalization of the expression for Bardeen–Cooper–Schrieffer superconductors with an isotropic in-plane gap function[26]. As the FS warping is rather small, $\Delta_{2D}(k_x, k_y)$ is approximately a constant. We expect this expression to be a good approximation, where η is a measure of the ratio of the interlayer to in-plane pairing strength. In Fig. 4b, we plot the measured Δ_{3D} on different FS sheets as a function of $\cos k_z$. To increase the accuracy, we used only the lower photon energy part of the gap dispersion and averaged over the left and right crossings. Figure 4b shows that equation (2) fits the data rather well, with the anisotropy ratios $\eta \sim 0.17$, 0.13 and -0.01 for the α, β and γ/δ bands, respectively (the gap values of the α' band are resolvable only near $k_z = \pi$). It is interesting to note that the values of η for the α and β bands are consistent with the ratio of the exchange coupling J_c/J_{ab} in the magnetically ordered parent compound, as extracted from the spin wave dispersion measured by neutron scattering[2], where $J_c \sim 5$ meV is the interlayer coupling and $J_{ab} \sim 30$ meV is the next-nearest-neighbour coupling in the Fe plane. Note that k-averaged J_c would have most contributions from the bands with appreciable k_z dispersion, such as α, α' and β hole-like bands.

The observation of the cosine dependence of the SC gap on k_x, k_y and k_z indicates that the gap function reflects the lattice symmetry and that the predominant pairing could be short-ranged in real space. Under such an assumption, and taking into account the lattice symmetry, the leading terms of a generalized s-wave gap function can be written as $\Delta_1 \cos k_x \cos k_y + (\Delta_2/2)(\cos k_x + \cos k_y)\cos k_z + \Delta_3(\cos k_x \cos k_y)\cos k_z$. It is possible that the gap parameters of Δ_1, Δ_2 and Δ_3 have some band/orbital dependence. For simplicity, we choose band/orbital-independent parameters to fit the data. We found that $\Delta_3 \ll \Delta_2$ as a result of the vanishingly small η of the γ/δ electron-like FS around $(\pi, 0)$.

Remarkably, the remaining terms $\Delta_1 \cos k_x \cos k_y + (\Delta_2/2)(\cos k_x + \cos k_y)\cos k_z$ fit all the gap values on the different FS sheets fairly well, with $\Delta_1 = 12.3$ meV and $\Delta_2 = 2.07$ meV, as shown in Fig. 4c. The ratio of Δ_2/Δ_1 is nearly the same as the ratio of J_c/J_{ab}. We have also checked that the SC gap on each observed FS sheet along different in-plane directions fits well to this 3D gap function.

Our finding of a single 3D superconducting gap function for all five different FS pockets indicates that there are only two dominant pairing energy scales, one in-plane and one out-of-plane, in pnictide superconductors. It points to a common origin for the pairing strengths on all the observed FS sheets, independent of their different density of states. Moreover, because this gap function can be obtained by decoupling the 3D next-nearest-neighbour antiferromagnetic exchange couplings within the pairing channel, our results are consistent with pairing induced by short-ranged antiferromagnetic fluctuations in the iron-pnictide superconductor[9,10,27].

Methods

We have carried out systematic photon-energy-dependent ARPES measurements in the superconducting state of the optimally hole-doped $Ba_{0.6}K_{0.4}Fe_2As_2$ superconductors ($T_c = 37$ K). The high-quality single crystals used in our study were grown by the flux method[28]. High-resolution ARPES measurements were conducted at the SIS beamline of the Swiss Light Source. The photon energy used in the experiments is between 20 and 110 eV, with different circular and linear polarization. The energy resolution is 8–20 meV depending on the photon energy, and the momentum resolution is below 0.02 Å^{-1}. Samples were cleaved *in situ* and measured at 10 K in a working vacuum better than 5×10^{-11} torr. The mirror-like sample surface was found to be stable, without obvious degradation during a typical measurement period of 24 h. Many samples have been measured and reproducible results have been obtained in these samples.

Received 24 August 2010; accepted 8 November 2010; published online 16 January 2011

References

1. Yuan, H. Q. *et al.* Nearly isotropic superconductivity in $(Ba,K)Fe_2As_2$. *Nature* **457,** 565–568 (2009).
2. Zhao, J. *et al.* Low energy spin waves and magnetic interactions in $SrFe_2As_2$. *Phys. Rev. Lett.* **101,** 167203 (2008).
3. Ding, H. *et al.* Observation of Fermi-surface-dependent nodeless superconducting gaps in $Ba_{0.6}K_{0.4}Fe_2As_2$. *Europhys. Lett.* **83,** 47001 (2008).
4. Zhao, L. *et al.* Multiple nodeless superconducting gaps in $(Ba_{0.6}K_{0.4})Fe_2As_2$ superconductor from angle-resolved photoemission spectroscopy. *Chin. Phys. Lett.* **25,** 4402–4405 (2008).
5. Wray, L. *et al.* Momentum-dependence of superconducting gap, strong-coupling dispersion kink, and tightly bound Cooper pairs in the high-T_c $(Sr,Ba)_{1-x}(K,Na)_xFe_2As_2$ superconductors. *Phys. Rev. B* **78,** 184508 (2008).
6. Nakayama, K. *et al.* Superconducting gap symmetry of $Ba_{0.6}K_{0.4}Fe_2As_2$ studies by angle-resolved photoemission spectroscopy. *Europhys. Lett.* **85,** 67002 (2009).
7. Mazin, I. I., Singh, D. J., Johannes, M. D. & Du, M. H. Unconventional superconductivity with a sign reversal in the order parameter of $LaFeAsO_{1-x}F_x$. *Phys. Rev. Lett.* **101,** 057003 (2008).
8. Kuroki, K. *et al.* Unconventional pairing originating from the disconnected Fermi surfaces of superconducting $LaFeAsO_{1-x}F_x$. *Phys. Rev. Lett.* **101,** 087004 (2008).
9. Seo, K., Bernevig, B. A. & Hu, J-P. Pairing symmetry in a two-orbital exchange coupling model of oxypnictides. *Phys. Rev. Lett.* **101,** 206404 (2008).
10. Wang, F. *et al.* Functional renormalization-group study of the pairing symmetry and pairing mechanism of the FeAs-based high-temperature superconductor. *Phys. Rev. Lett.* **102,** 047005 (2009).
11. Cvetkovic, V. & Tesanovic, Z. Multiband magnetism and superconductivity in Fe-based compounds. *Europhys. Lett.* **85,** 37002 (2009).
12. Fletcher, J. D. *et al.* Evidence for a nodal-line superconducting state in LaFePO. *Phys. Rev. Lett.* **102,** 147001 (2009).
13. Nakai, Y. *et al.* ^{31}P and ^{75}As NMR evidence for a residual density of states at zero energy in superconducting $BaFe_2(As_{0.67}P_{0.33})_2$. *Phys. Rev. B* **81,** 020503(R) (2010).
14. Reid, J-Ph. *et al.* Nodes in the gap structure of the iron arsenide superconductor $Ba(Fe_{1-x}Co_x)_2As_2$ from *c*-axis heat transport measurements. *Phys. Rev. B* **82,** 064501 (2010).
15. Hüfner, S. *Photoelectron Spectrsoscopy* (Springer, 1995).
16. Vilmercati, P. *et al.* Evidence for three-dimensional Fermi-surface topology of the layered electron-doped iron superconductor $Ba(Fe_{1-x}Co_x)_2As_2$. *Phys. Rev. B* **79,** 220503(R) (2009).
17. Liu, C. *et al.* Three- to two-dimensional transition of the electronic structure in $CaFe_2As_2$: A parent compound for an iron arsenic high-temperature superconductor. *Phys. Rev. Lett.* **102,** 167004 (2009).
18. Malaeb, W. *et al.* Three-dimensional electronic structure of superconducting iron pnictides observed by angle-resolved photoemission spectroscopy. *J. Phys. Soc. Jpn.* **78,** 123706 (2009).
19. Brouet, V. *et al.* Nesting between hole and electron pockets in $Ba(Fe_{1-x}Co_x)_2As_2$ ($x = 0$–0.3) observed with angle-resolved photoemission. *Phys. Rev. B* **80,** 165115 (2009).
20. Thirupathaiah, S. *et al.* Orbital character variation of the Fermi surface and doping dependent changes of the dimensionality in $BaFe_{2-x}Co_xAs_2$ from angle-resolved photoemission spectroscopy. *Phys. Rev. B* **81,** 104512 (2010).
21. Singh, D. J. & Du, M. H. Density functional study of $LaFeAsO_{1-x}F_x$: A low carrier density superconductor near itinerant magnetism. *Phys. Rev. Lett.* **100,** 237003 (2008).
22. Ma, F. & Lu, Z-Y. Iron-based layered compound LaFeAsO is an antiferromagnetic semimetal. *Phys. Rev. B* **78,** 033111 (2008).
23. Xu, G., Zhang, H., Dai, X. & Fang, Z. Electron–hole asymmetry and quantum critical point in hole-doped $BaFe_2As_2$. *Europhys. Lett.* **84,** 67015 (2008).
24. Rotter, M., Tegel, M. & Johrendt, D. Superconductivity at 38 K in the iron arsenide $(Ba_{1-x}K_x)Fe_2As_2$. *Phys. Rev. Lett.* **101,** 107006 (2008).
25. Graser, S. *et al.* Spin fluctuations and superconductivity in a three-dimensional tight-binding model for $BaFe_2As_2$. *Phys. Rev. B* **81,** 214503 (2010).
26. Bulaevskii, L. N. & Zyskin, M. V. Energy gap in layered superconductors. *Phys. Rev. B* **42,** 10230 (1990).
27. Si, Q. & Abrahams, E. Strong correlations and magnetic frustration in the high T_c iron pnictides. *Phys. Rev. Lett.* **101,** 076401 (2008).
28. Chen, G. F. *et al.* Transport and anisotropy in single-crystalline $SrFe_2As_2$ and $A_{0.6}K_{0.4}Fe_2As_2$ (A = Sr, Ba) superconductors. *Phys. Rev. B* **78,** 224512 (2008).

Acknowledgements

We thank X. Dai, B. A. Bernevig and Z. Fang for valuable discussions. This work was supported by grants from the Chinese Academy of Sciences, NSF, the Ministry of Science and Technology of China, NSF, DOE of US, and the Sino-Swiss Science and Technology Cooperation.

Author contributions

Y-M.X., Y-B.H., X-Y.C., E.R. and M.R. carried out the experiments. Y-M.X. and Y-B.H. analysed the data. H.D., Y-M.X., J-P.H. and Z.W. designed the experiments. Z.W., H.D., Y-M.X. and J-P.H. wrote the paper. G-F.C., P.Z., N-L.W., C-L.Z. and P-C.D. synthesized materials. All authors discussed the results and commented on the manuscript.

Additional information

The authors declare no competing financial interests. Reprints and permissions information is available online at http://npg.nature.com/reprintsandpermissions. Correspondence and requests for materials should be addressed to H.D.